



ATR-FTIR spectroscopic characterization of ferric arsenic-containing colloid and gypsum

Lijun Fan, Xiongjian Zhang*

College of Geoscience and Surveying Engineering, China University of Mining & Technology, Beijing 100083, China, email: tbp1600201033@student.cumtb.edu.cn (L. Fan), 406483672@qq.com (X. Zhang)

Received 5 September 2018; Accepted 1 January 2019

ABSTRACT

This study chose a typical arsenic and iron-containing sediments sampled from the Shimen realgar mine for the purpose of investigating the centrifugation on the separation of the colloid and crystalline components. The effect was characterized by using an *in-situ* attenuated total reflection Fourier transform infrared (ATR-FTIR) spectroscopic method. The sediments were firstly characterized by XRD, SEM-EDX, XPS and *in-situ* FTIR. XRD and SEM results showed that the sediments were made of arsenic iron-containing colloid and crystalline gypsum. Infrared bands at 790 and 872 cm^{-1} were assigned to the symmetric stretching vibrations of As-O. The binding energy of XPS for Fe_{2p} and As_{3d} were 713 and 45 eV, respectively, indicating the Fe was trivalent and As was pentavalent. Then, the colloid and crystalline components were separated by different centrifugal speeds (from 0 to 11000 rpm). Obvious increase in the characteristic peak intensity at 1113 cm^{-1} with increasing centrifugal speed was observed. Centrifugation at 8000 rpm was the best threshold to separate the colloid and gypsum. Therefore, centrifugation combined with ATR-FTIR spectroscopic technique might be regarded as a feasible mean to give both quantitative and qualitative information on the separation performance, which might be benefit to reduce mine wastes and establish a feasible pre-treatment scheme for future arsenic treatment.

Keywords: Arsenic; Colloid; Gypsum; Centrifugation; ATR-FTIR

1. Introduction

Arsenic (As) pollution was found worldwide in acid mine drainage (AMD) due to extensive gold, silver *etc.* mine exploitation and its relevant treatments [1]. The dissolution of kinds of iron- and arsenic-bearing sulfide minerals, such as arsenopyrite (FeAsS), realgar (AsS), orpiment (As_2S_3) can release quantities of arsenic, iron or sulfate into diverse system [2,3]. Then, newly-formed dissolved ferric ions can easily form inorganic colloids with arsenic, which can greatly influence arsenic dynamics in supergene environments [4–6].

Realgar (AsS) is one common arsenic sulfide. Shimen realgar mine was once the biggest realgar mine in Asia, which had mining activities for more than one thousand years. This realgar deposit was formed by shallow low-tem-

perature hydrothermal veins. In Chinese history, realgar was once used as traditional medicine to treat a wide range of diseases. Compendium of Material Medica written by Li Shizhen in Ming Dynasty recorded that it can be used to fight against skin diseases like herpes, sores. Realgar was also added into liqueur on the Chinese traditional Dragon Boat Festival, which delivered some wishes to resist various toxins. Nowadays, intensive exploitation of realgar ore, leading to quantities release of arsenic into water and soil, is widely believed to be the main reason of arsenic contamination in this region. At last half century, ferric sulfate ($\text{Fe}_2(\text{SO}_4)_3$) and lime (CaO) were both used to treat the acid water from Shimen realgar mine when processed realgar mining wastes.

Dissolved Ca^{2+} and SO_4^{2-} from ferric sulfate, or the oxidization of reduced S^{2-} of realgar, can form secondary gypsum ($\text{CaSO}_4 \cdot 2\text{H}_2\text{O}$), which is one common by-product in pyrometallurgy and hydrometallurgy operations. Arse-

*Corresponding author.

nic can be incorporated into these secondary minerals. The transformation and stability of these secondary arsenic phases had been widely investigated in Ca-Fe-AsO₄-SO₄ system [1,2]. Large quantities of phosphogypsum were also found during phosphate fertilizer production. Due to the geochemical similarity between phosphorus and arsenic, the incorporation of arsenic into gypsum was recently studied in mineralogy in terms of mineral trap for contaminants [3,4]. Therefore, the removal of gypsum is an important consideration for further arsenic remediation.

The previous investigation showed large quantities of ferric arsenic-containing sediments were deposited in Shimen realgar mine. The objective of this study is to investigate the centrifugation separate effect of the colloid and crystalline component (gypsum) by using *in-situ* ATR-FTIR to characterize. Centrifugation is a commonly applied separation method based on density variation which can separate the colloid and crystalline gypsum effectively [5,6]. The difference in separation can theoretically be observed and characterized by spectroscopic band. In addition, there have been some studies using Infrared Spectroscopic (IR) method to quantitative characterize the mineral abundances of clay-gypsum mixtures [7,8]. Therefore, *in-situ* ATR-FTIR might can be used to characterize the separation performance.

This study firstly characterized the ferric sediments collected from Shimen realgar mine by spectroscopic mean, then attempt to separate the colloid and crystalline components by centrifugation. The corresponding component variations were described in characterized band by *in-situ* ATR-FTIR. These work might be used to afford help to reduce mine wastes and establish a feasible pre-treatment scheme for future arsenic treatment.

2. Experiment and method

2.1. Sediments sampling and characterization

The Shimen realgar mine site is located in Changde City, Hunan province in central south China, which is famous for abundant realgar ore deposit worldwide [9–11]. The sediments used in this study were derived from an abandoned tailing dam. They were collected directly by hand wearing a plastic glove and immediately put into an epoxy-lined plastic can and transported into the lab within 2 d (Fig. 1). The



Fig. 1. Raw sediments from Shimen Realgar mine area.

upper water of the sediments was passed through a 0.22 μm cellulose membrane for the ion concentration analysis. The cations (Ca, Fe, As, Al, Sb, Se, K, Mn, Mg, Si, U) and SO₄²⁻ were analyzed by Inductive Coupled Plasma Emission Spectrometry (ICP-AES, iCAP6500 Thermo Fisher) and Ion chromatography (IC, Metrohm, 881 Compact pro). The pH was measured using a pH meter (PB-21, Sartorius). The sediments were kept in a refrigerator at 4°C and then freeze-dried under vacuum environment (LABCONCO, FreeZone) and sieved to less than 100 mesh for later characterize using XRD and SEM-EDX. X-ray diffraction (XRD) patterns were recorded using an X' Pert PRO (PANalytical, Netherland) instrument with a Cu-Kα source. Diffraction data were acquired over a 2θ range of 10–80° with a scan time of 10.16 s per step and a step size of 0.03°. The surface morphology was imaged using scanning electron microscopy (SEM, EVO@18, ZEISS) equipped with energy-dispersive-X-ray-spectroscopy (EDX) operating at 15 kV.

2.2. Fourier Transform Infrared Spectroscopy (FTIR) characterization of sediments

Infrared spectroscopy of the sediments and colloid suspensions were analyzed by a Perkin-Elmer Spectrum Fourier Transform Infrared Spectroscopy (ATR-FTIR, Frontier) coupled with a diamond and six-reflection horizontal ZnSe Attenuated Total Reflection (ATR, Geteway, specac) accessory, respectively. Due to the larger area of the ZnSe crystal top plate than diamond accessory, this pattern may yield reproducible films in good and uniform contact with ATR crystal. The colloid films were directly deposited on the clean 45° ZnSe crystal internal reflection element (70×10 mm) installed in the Frontier spectrometer. Throughout the experiment, the sediments FTIR and colloid single beam ATR-FTIR spectra were collected in a range of 400–4000 cm⁻¹ and 650–1500 cm⁻¹ respectively, with a spectral resolution of 1 cm⁻¹ and 64 scans.

2.3. X-ray photoelectron spectroscopy (XPS) characterization of sediments

To understand the valance of Fe and As in the raw sediments, X-ray photoelectron spectroscopy (XPS) was used. The Al-Kα line was used as radiation source, and the survey spectra were obtained with a VG-ScientaR3000 analyzer pass energy of 30 eV.

2.4. Preparation of colloid-suspension and characterization

The freshly ferric arsenic-containing colloid suspensions were prepared by making a slurry of 50 mg sample in 50 ml milli-Q water in the polypropylene vial, homogenized by shaking, and ultrasonicated for 30 min to separate the colloid from crystal, then centrifuged at 0, 4000, 8000, 10,000 11000 rpm for 10 min (Eppendorf, Centrifuge 5804 R), respectively. Then, a uniformly layered suspension can be formed. Two mL supernatant was recovered immediately and spread over a clean and dry ZnSe ATR crystal and then dried overnight in air at room temperature, forming an even film on the ATR crystal surface. Fig. 2 shows the sketch of the preparation of colloid-suspension films. All experi-

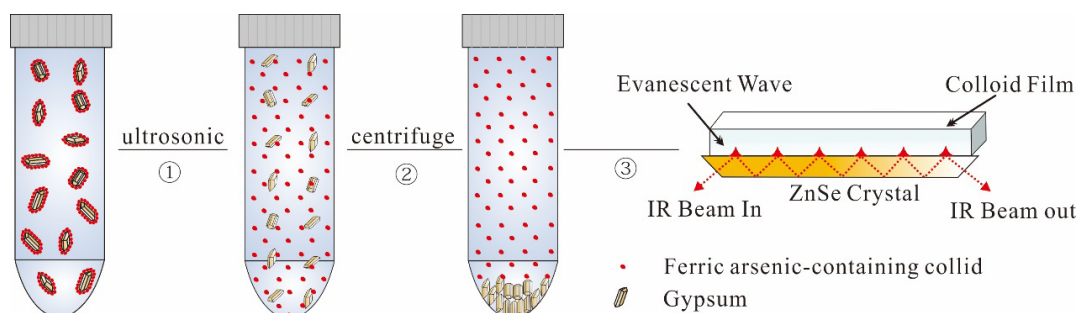


Fig. 2. The preparation process of colloid-suspension films.

ments were conducted in duplicates and the averages were obtained to avoid the variation of the film thickness.

2.5. Size characterization and elemental quantification of colloid-suspension

The particle size distribution of colloid suspensions was determined by a Laser Particle Size Analyzer (LS13320, no data were shown). The colloid suspensions were passed through 0.22 μm filters and analyzed for the main cations determined by Inductively-Coupled Plasma-Optical Spectroscopy (ICP-AES, iCAP 6500, ThermoFisher).

3. Results and discussion

3.1. Characterization of sediment

The XRD results are in Fig. 3. It shows that the sample has good crystallinity and its diffraction lines matched very well with gypsum (PDF 21-0816). There were also some features of amorphous phase on the XRD patterns indicating the sediments contained some amorphous materials. The analysis showed that it was similar to schwertmannite (PDF 47-1775).

The SEM images presented in Fig. 4 (A, B) also show that the sediments were made of amorphous and crystalline materials. The EDX results (Figs. 4C, D) confirmed that the crystal material was gypsum, which was acicular crystal. Another amorphous material was cotton-like, which deposited on the gypsum surface. The elements analysis of EDX showed that these amorphous materials contained As and Fe. The chemical ions analysis of upper water layer of this sediment showed that As, Ca, Mg, K, Si and SO_4^{2-} concentrations were 0.40, 410.7, 13.7, 3.8, 2.0 and 401.8 mg/L, whereas Al, Sb, Se and U concentrations were less than 0.01 mg/L. Long-term water-rock interaction resulted in arsenate incorporated into the structure of these amorphous ferric colloid. Many studies indicated that arsenic can be incorporated into ferric minerals or gypsum structure or adsorbed by ferric minerals [12–14]. Thus, Fe(III)(oxy)hydroxides like schwertmannite, ferrihydrite, hematite can be used as effective adsorbents for arsenic removal [15–18]. However, no As was detected in the gypsum crystal in the raw sediments we sampled.

3.2. XPS analysis

The XPS spectra of Fe 2p and As 3d of the sediments were shown in Fig. 5, the binding energies for the compo-

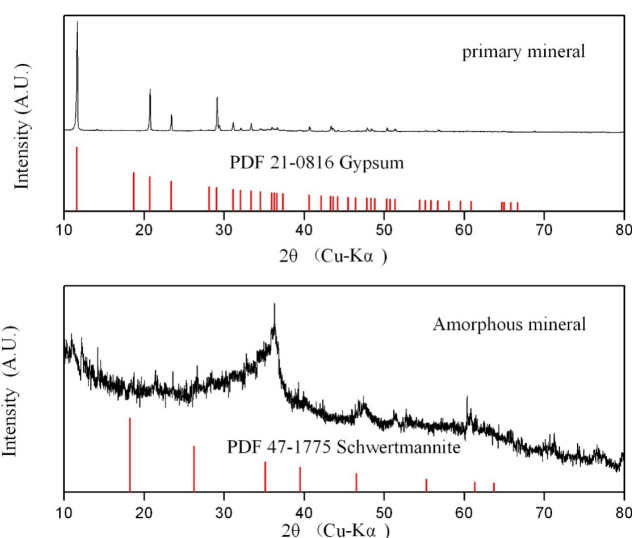


Fig. 3. Powder XRD patterns of the sediments.

nents peaks of Fe and As were identified by comparing to the reported values [19,20]. The Fe_{2p} and As_{3d} peaks at 712.99 eV (Fig. 5A) and 44.88 eV (Fig. 5B) showed that the valence of Fe and As were consistent with previously reported for Fe(III) and As(V). Some research had shown that the exist of reductive bacteria could result in arsenic release and valence variation of As/Fe in the sediments [21,22]. Future arsenic species variation during the sediments dissolution in this area by native reducing bacteria will be investigated.

3.3. ATR-FTIR analysis

The infrared spectrum of the sample is shown in Fig. 6. The wavenumbers region of interest, i.e. the stretching and bending vibration regions of As-O ($730\text{--}930\text{ cm}^{-1}$), the S-O bonds ($500\text{--}1250\text{ cm}^{-1}$), and the water HOH/OH vibration region ($1000\text{--}4000\text{ cm}^{-1}$) were displayed. The band at 790 cm^{-1} and 872 cm^{-1} were assigned to the symmetric stretching vibration of As-O [14]. The strong band peaking at 1113 cm^{-1} was assigned to S-O symmetric stretching vibration (ν_1) of sulfate, while the 666 cm^{-1} and 601 cm^{-1} were assigned to S-O in-plane bending vibrations (ν_4). The presence of water in the sample can be detected and characterized by peaks in spectral region near 3500 cm^{-1} and 1600 cm^{-1} . The

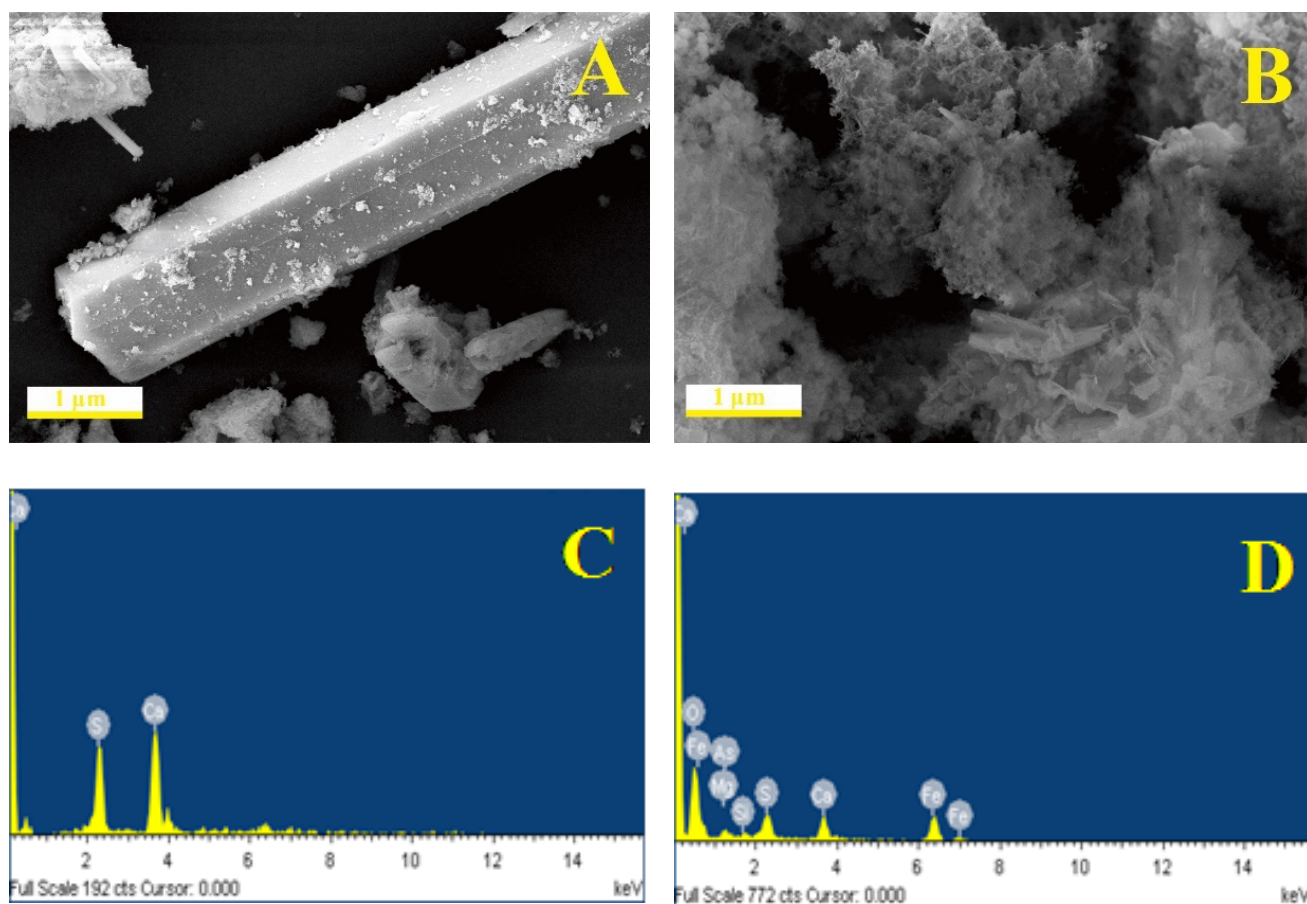


Fig. 4. The SEM (A, B) and EDX (C, D) images.

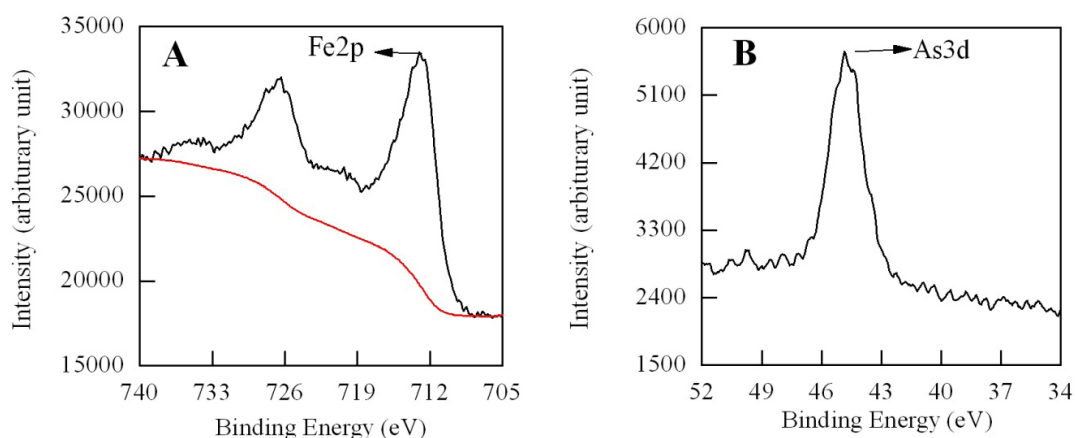


Fig. 5. The XPS spectra of Fe 2p and As 3d for the sample.

peaks at 3395 cm^{-1} and 3489 cm^{-1} were symmetric stretching vibration (ν_1) and antisymmetric (ν_3) stretching vibration of HOH. The two peaks at 1683 and 1619 cm^{-1} were for O-H bending vibration (ν_2), which were identical to the bands of gypsum ($\text{CaSO}_4 \cdot 2\text{H}_2\text{O}$) [23]. The peak at 1453 cm^{-1} may be due to adsorption of moisture. This atmospheric moisture can be easily absorbed by the pellet in recording IR spectra bands belong to O-H bending mode [24].

The aqueous phase ATR-FTIR spectra of colloid-suspensions were collected as a function of different centrifugal speed. In this paper, the centrifuge speed refers to the revolutions per minute. The colloid films were analyzed by *in-situ* ATR-FTIR at different revolutions per minute (0, 4000, 8000, 10000, 11000 rpm) under ambient atmospheric condition. There were obvious changes in characteristic peak intensity at 1113 cm^{-1} with increasing centrifugal speed in

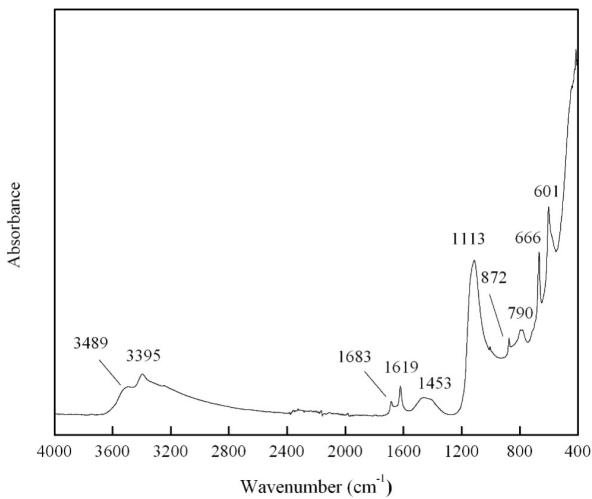


Fig. 6. The ATR-FTIR spectra of sample from 4000 to 400 cm^{-1} .

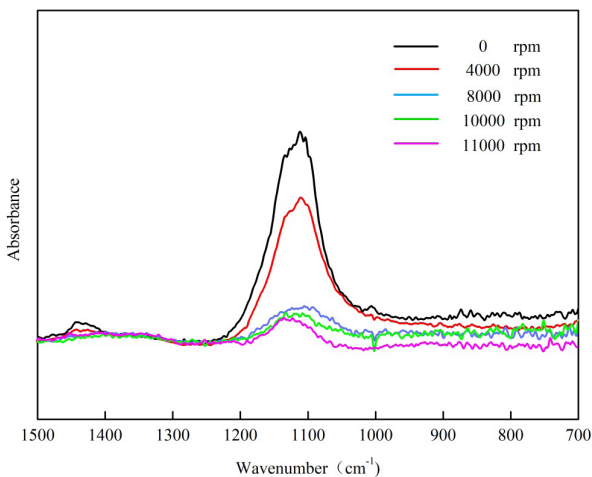


Fig. 7. In situ ATR-FTIR spectra of colloid suspensions with centrifugal speeds from 0 to 11000 rpm.

Fig. 7. The peak change in the range of 1109–1126 cm^{-1} were assigned to sulfate groups presented in colloid films, the peak intensity indicated the content change of sulfate. As the centrifugal speed increased from 0 to 8000 rpm, the S-O stretching vibration band dropped sharply, while from 8000 to 11000 rpm, the intensity of S-O band decreased slightly. This phenomenon indicated that amorphous ferric arsenic-containing minerals and gypsum could be separated by centrifugation. The 8000 rpm was likely the best threshold to separate them, while the other centrifugal speeds (0, 4000, 10000, 11000 rpm) did not present better separation performance. Meanwhile, arsenic concentrations of supernatant for corresponding centrifugal speeds were 0.25 (4000 rpm), 0.23 (8000 rpm), 0.23 (10000 rpm) and 0.23 (11000 rpm) mg/L, respectively, indicating the arsenical colloid concentration may not vary obviously. The calcium concentrations plateaued at 161.4 (4000 rpm), 170.8 (8000 rpm), 171.5 (10000 rpm) and 170.3 (11000 rpm) mg/L. The reason for this might be the different centralized distribution sizes

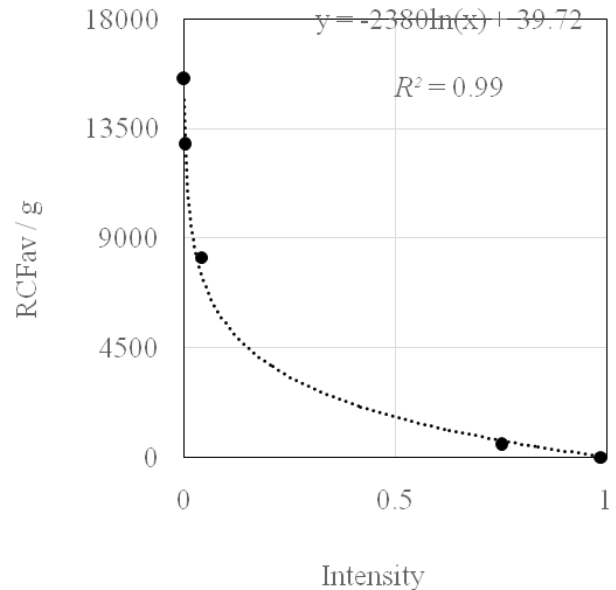


Fig. 8. The relationship diagram between infrared intensity and relative centrifuge force.

of crystal gypsum and colloidal ferric arsenic-containing minerals. It was probably ascribed that density different of these two components at various centrifugal speeds, which could obviously be reflected in *in-situ* ATR-FTIR spectra.

Different centrifugal speeds represent different relative centrifugal force (RCF) which is the acceleration measured in multiples of the gravitational acceleration constant, g . Meanwhile, RCF can be calculated according to the following equations:

$$RCF = 1.12r(\text{rpm} / 1000)^2 \quad (1)$$

$$\text{rpm} = 1000\sqrt{RCF / 1.12r} \quad (2)$$

where RCF is the Relative Centrifugal Force (g); rpm is the revolutions per minute; r is the radius of gyration (mm).

Accordingly, the relationship between relative centrifugal force and peak intensity of characteristic bands from colloidal ferric arsenic-containing minerals can be obtained. The regression value (R^2) was 0.99. It is possible to separate ferric arsenic-containing colloid and gypsum according to rpm. So, centrifugation is useful to reduce gypsum for the pre-treatment of the large quantities of arsenical gypsum. The infrared characterization is a rapid and feasible method to determine this separation.

4. Conclusion

The arsenic and iron-containing gypsum sediments from the Shimen realgar mine area had been characterized firstly based on spectroscopic means. The sediments mainly contained of colloidal arsenic and crystalline gypsum. The *in-situ* ATR-FTIR spectroscopy is likely a powerful method to study the separation performance between colloid and crystalline gypsum. Obvious change in characteristic peak

intensity at 1113 cm^{-1} with increasing centrifugal speed was observed. Centrifugation of 8000 rpm was the best threshold to separate the colloid and gypsum. In addition, the relation between Relative Centrifugation Force (RCF, Y) and peak intensity of infrared bands at 1113 cm^{-1} (X) followed the equation of $Y = -2380 \cdot \ln(x) + 39.72$. Therefore, centrifugation combined with ATR-FTIR spectroscopic technique might be regarded as a feasible and effective mean to give both quantitative and qualitative information on the separation performance, which might be useful to help reduce the enormous arsenic-containing mine wastes in Shimen realgar mine.

Acknowledgments

This study was supported by the National Natural Science Foundation of China (Grant No. 41372051) and the joint Research Project between China and South Africa from Ministry of Science and Technology of China (2012DFG71060).

References

- [1] S. Das, J. Essilfie-Dughan, M.J. Hendry, Fate of adsorbed arsenate during phase transformation of ferrihydrite in the presence of gypsum and alkaline conditions, *Chem. Geol.*, 411 (2015) 69–80.
- [2] M.A. Gomez, L. Becze, J.N. Cutler, G.P. Demopoulos, Hydrothermal reaction chemistry and characterization of ferric arsenate phases precipitated from $\text{Fe}_2(\text{SO}_4)_3\text{-As}_2\text{O}_5\text{-H}_2\text{SO}_4$ solutions, *Hydrometallurgy*, 107 (2011) 74–90.
- [3] L. Fan, F. Zhao, J. Liu, K.A. Hudson-Edwards, The As behavior of natural arsenical-containing colloidal ferric oxyhydroxide reacted with sulfate reducing bacteria, *Chemosphere*, 209 (2018) 381–391.
- [4] X. Turrillas, L. Charlet, M.R. Johnson, F. Bardelli, Arsenic uptake by gypsum and calcite: Modeling and probing by neutron and x-ray scattering, *Physica B*, 385 (2007) 935–937.
- [5] Z. Liu, Z.S. Carroll, S.C. Long, A. Roaespinoza, T. Runge, Centrifuge separation effect on bacterial indicator reduction in dairy manure, *J. Environ. Eng.*, 191 (2017) 268–274.
- [6] M. Hjorth, K.V. Christensen, M.L. Christensen, S.G. Sommer, Solid-liquid separation of animal slurry in theory and practice. A review, *Agron. Sustain. Dev.*, 30 (2010) 153–180.
- [7] K.M. Robertson, R.E. Milliken, S. Li, Estimating mineral abundances of clay and gypsum mixtures using radiative transfer models applied to visible-near infrared reflectance spectra, *Lcarus*, 277 (2016) 171–186.
- [8] Pitman, K.M. Dobrea, E.Z.N. Jamieson, C.S. Dalton, J.B. Abbey, W.J. Joseph, C.S. Emily, What Lurks in the Martian Rocks and Soil? Investigations of Sulfates, Phosphates, and Perchlorates. Reflectance spectroscopy and optical functions for hydrated Fe-sulfates, *Am. Mineral.*, 99 (2014) 1593–1603.
- [9] J. Tang, Y. Liao, Z. Yang, L. Chai, Characterization of arsenic serious-contaminated soils from Shimen realgar mine area, the Asian largest realgar deposit in China, *J. Soils Sediments*, 16 (2016) 1519–1528.
- [10] X. Zhu, R. Wang, L.U. Xiancai, Secondary minerals of weathered orpiment-realgar-bearing tailings in shimen carbonate-type realgar mine, Changde, Central China, *Min. Petrol.*, 109 (2013) 1–15.
- [11] Y. Wu, X.Y. Zhou, M. Lei, J. Yang, J. Ma, P.W. Qiao, T.B. Chen, Migration and transformation of arsenic: Contamination control and remediation in realgar mining areas, *Appl. Geochem.*, (2016) 44–51.
- [12] E.D. Burton, R.T. Bush, S.G. Johnston, K.M. Watling, R.K. Hocking, L.A. Sullivan, G.K. Parker, Sorption of arsenic(V) and arsenic(III) to schwertmannite, *Environ. Sci. Technol.*, 43 (2009) 9202–9207.
- [13] R.S. Cutting, V.S. Coker, N.D. Telling, R.L. Kimber, G.V.D. Laan, R.A.D. Patrick, D.J. Vaughan, E. Arenholz, J.R. Lloyd, Microbial reduction of arsenic-doped schwertmannite by *Geobacter sulfurreducens*, *Environ. Sci. Technol.*, 46 (2012) 12591–12599.
- [14] D. Zhang, Z. Yuan, S. Wang, Y. Jia, G.P. Demopoulos, Incorporation of arsenic into gypsum: Relevant to arsenic removal and immobilization process in hydrometallurgical industry, *J. Hazard. Mater.*, 300 (2015) 272–280.
- [15] Z. Yang, Z. Wu, Y. Liao, L. Qi, W. Yang, L. Chai, Combination of microbial oxidation and biogenic schwertmannite immobilization: A potential remediation for highly arsenic-contaminated soil, *Chemosphere*, 181 (2017) 1–8.
- [16] L. Carlson, J.M. Bigam, U. Schwertmann, A. Kyek, F. Wagner, Scavenging of As from acid mine drainage by schwertmannite and ferrihydrite: a comparison with synthetic analogues, *Environ. Sci. Technol.*, 36 (2002) 1712–1719.
- [17] Y. Jia, G.P. Demopoulos, Adsorption of arsenate onto ferrihydrite from aqueous solution: influence of media (sulfate vs nitrate), added gypsum, and pH alteration, *Environ. Sci. Technol.*, 39 (2005) 9523–9527.
- [18] L. Fan, F. Zhao, J. Liu, R. L. Frost, The As behavior of natural arsenical-containing colloidal ferric oxyhydroxide reacted with sulfate reducing bacteria, *Chem. Eng. J.*, 332 (2018) 183–191.
- [19] T. Yamashita, P. Hayes, Analysis of XPS spectra of Fe^{2+} and Fe^{3+} ions in oxide materials, *Appl. Surf. Sci.*, 254 (2008) 2441–2449.
- [20] J.L. Liang, W.D. Sun, Y.L. Li, S.Y. Zhu, H. Li, Y.L. Liu, W. Zhai, An XPS study on the valence states of arsenic in arsenian pyrite: Implications for Au deposition mechanism of the Yangshan Carlin-type gold deposit, western Qinling belt, *J. Asian Earth Sci.*, 62 (2013) 363–372.
- [21] J. Zobrist, P.R. Dowdle, J.A.D. And, R.S. Oremland, Mobilization of Arsenite by dissimilatory reduction of adsorbed Arsenate mobilization of Arsenite by dissimilatory reduction of adsorbed Arsenate, *Environ. Sci. Technol.*, 34 (2000) 4747–4753.
- [22] L. Xu, Z. Zhao, S. Wang, R. Pan, Y. Jia, Transformation of arsenic in offshore sediment under the impact of anaerobic microbial activities, *Water Res.*, 45 (2011) 6781–6788.
- [23] Y. Liu, A. Wang, J. Freeman, Raman, MIR, and NIR spectroscopic study of calcium sulfates: gypsum, bassanite, and anhydrite, in: *Lunar and Planetary Science Conference*, 2009, 2128.
- [24] M.R. Ahsan, M.A. Uddin, M.G. Mortuza, Infrared study of the effect of P2O5 in the structure of lead silicate glasses, *Indian J. Pure Ap. Phys.*, 43 (2005) 89–99.